The Nucleosomal Surface as a Docking Station for Kaposi's Sarcoma Herpesvirus LANA

Andrew J. Barbera *et al.*

Science **311**, 856 (2006);
DOI: 10.1126/science.1120541

they will seem to display regarding their musical preferences; thus the characteristics of success will seem predictable in retrospect. On the other hand, looking across different realizations of the same process, we see that as social influence increases (i.e., from experiment 1 to experiment 2), which particular products turn out to be regarded as good or bad becomes increasingly unpredictable, whether unpredictability is measured directly (Fig. 2) or in terms of quality (Fig. 3). We conjecture, therefore, that experts fail to predict success not because they are incompetent judges or misinformed about the preferences of others, but because when individual decisions are subject to social influence, markets do not simply aggregate pre-existing individual preferences. In such a world, there are inherent limits on the predictability of outcomes, irrespective of how much skill or information one has.

Although Web-based experiments of the kind used here are more difficult to control in some respects than are experiments conducted in physical laboratories (*18*), they have an important methodological advantage for studying collective social processes like cultural market formation. Whereas experimental psychology, for example, tends to view the individual as the relevant unit of analysis, we are explicitly interested in the relationship between individual (micro) and collective (macro) behavior; thus we need many more participants. In order to ensure that our respective worlds had reached reasonably steady states, we required over 14,000 participants—a number that can be handled easily in a Web-based experiment, but which would be impractical to accommodate in a physical laboratory. Because this "micro-macro" feature of our experiment is central to all collective social dynamics (*23*), we anticipate that Web-based experiments will become increasingly useful to the study of social processes in general.

References and Notes

1. H. L. Vogel, *Entertainment Industry Economics* (Cambridge Univ. Press, Cambridge, UK, 2004).
2. A. B. Krueger, *J. Labor Econ.* **23**, 1 (2005).
3. K. H. Chung, R. A. K. Cox, *Rev. Econ. Stat.* **76**, 771 (1994).
4. A. De Vany, *Hollywood Economics* (Routledge, London, 2004).
5. P. M. Hirsch, *Am. J. Sociology* **77**, 639 (1972).
6. W. T. Bielby, D. D. Bielby, *Am. J. Sociology* **99**, 1287 (1994).
7. R. E. Caves, *Creative Industries* (Harvard Univ. Press, Cambridge, MA, 2000).
8. R. A. Peterson, D. G. Berger, *Admin. Sci. Quart.* **16**, 97 (1971).
9. S. Rosen, *Am. Econ. Rev.* **71**, 845 (1981).
10. R. H. Frank, P. J. Cook, *The Winner-Take-All Society* (Free Press, New York, NY, 1995).
11. R. Bond, P. B. Smith, *Psychol. Bull.* **119**, 111 (1996).
12. R. B. Cialdini, N. J. Goldstein, *Annual Rev. Psych.* **55**, 591 (2004).
13. D. J. Watts, *Proc. Natl. Acad. Sci. U.S.A.* **99**, 5766 (2002).
14. P. Hedström, in *Social Mechanisms: An Analytical Approach to Social Theory*, P. Hedström, R. Swedberg, Eds. (Cambridge Univ. Press, Cambridge, UK, 1998), pp. 306–327.
15. M. Adler, *Am. Econ. Rev.* **75**, 208 (1985).
16. Available at (http://musiclab.columbia.edu).
17. Available at (http://bolt.com).
18. Materials and methods are available as supporting material on *Science* Online.
19. P. D. Allison, *Am. Sociol. Rev.* **43**, 865 (1978).
20. S. Bikhchandani, D. Hirshleifer, I. Welch, *J. Pol. Econ.* **100**, 992 (1992).
21. L. R. Anderson, C. A. Holt, *Am. Econ. Rev.* **87**, 847 (1997).
22. D. Kübler, G. Weizsäcker, *Rev. Econ. Stud.* **71**, 425 (2004).
23. J. S. Coleman, *Foundations of Social Theory* (Harvard Univ. Press, Cambridge, MA, 1990).

24. We thank P. Hausel for developing the MusicLab Web site; J. Booher-Jennings for design work; S. Hasker for helpful conversations; and A. Cohen, B. Thomas, and D. Arnold at Bolt Media for their assistance in recruiting participants. Supported in part by an NSF Graduate Research Fellowship (to M.J.S.), NSF grants SES-0094162 and SES-0339023, the McDonnell Foundation, and Legg Mason Funds.

Supporting Online Material

www.sciencemag.org/cgi/content/full/311/5762/854/DC1
Materials and Methods
SOM Text
Figs. S1 to S10
Tables S1 to S4
References

6 October 2005; accepted 22 December 2005
10.1126/science.1121066

The Nucleosomal Surface as a Docking Station for Kaposi's Sarcoma Herpesvirus LANA

Andrew J. Barbera,[1]* Jayanth V. Chodaparambil,[2]* Brenna Kelley-Clarke,[1] Vladimir Joukov,[3] Johannes C. Walter,[4] Karolin Luger,[2] Kenneth M. Kaye[1]†

Kaposi's sarcoma–associated herpesvirus (KSHV) latency-associated nuclear antigen (LANA) mediates viral genome attachment to mitotic chromosomes. We find that N-terminal LANA docks onto chromosomes by binding nucleosomes through the folded region of histones H2A-H2B. The same LANA residues were required for both H2A-H2B binding and chromosome association. Further, LANA did not bind *Xenopus* sperm chromatin, which is deficient in H2A-H2B; chromatin binding was rescued after assembly of nucleosomes containing H2A-H2B. We also describe the 2.9-angstrom crystal structure of a nucleosome complexed with the first 23 LANA amino acids. The LANA peptide forms a hairpin that interacts exclusively with an acidic H2A-H2B region that is implicated in the formation of higher order chromatin structure. Our findings present a paradigm for how nucleosomes may serve as binding platforms for viral and cellular proteins and reveal a previously unknown mechanism for KSHV latency.

Kaposi's sarcoma–associated herpesvirus (KSHV) has an etiological role in Kaposi's sarcoma (KS), the predominant AIDS malignancy; primary effusion lymphoma (PEL); and multicentric Castleman's disease (*1*–*4*). KSHV persists as a multicopy episome in latently infected tumor cells (*5*, *6*). Viral genomes lack centromeres, which govern faithful DNA partitioning in eukaryotic cells, and use a distinct segregation mechanism in which the 1162–amino acid KSHV latency-associated nuclear antigen (LANA) tethers episomes to mitotic chromosomes. LANA is required for episome persistence, and interaction with mitotic chromosomes is essential for its function. The first 22 residues comprise the dominant LANA chromosome-association region, because the C-terminal chromosome targeting domain is unable to rescue chromosome association in mutants that are deleted for or contain specific mutations within the N-terminal region (*7*–*10*). We therefore sought to determine the chromosome docking partner of the LANA N terminus.

Genetic analysis of LANA's chromosome binding region was central to our strategy for characterization of putative docking partners. Transient assays have shown that alanine substitutions at LANA residues 5 to 7 [original amino acids were GMR (*11*)], 8 to 10 (originally LRS), or 11 to 13 (originally GRS) (termed LANA $_{5}$GMR$_{7}$, LANA $_{8}$LRS$_{10}$, and LANA $_{11}$GRS$_{13}$, respectively) (Fig. 1A) lack chromosome association, whereas LANA with alanine substitutions at amino acids 17 to 19 (originally PLT) or 20 to 22 (originally RGS) (termed LANA $_{17}$PLT$_{19}$ and LANA $_{20}$RGS$_{22}$,

[1]Channing Laboratory, Department of Medicine, Brigham and Women's Hospital, Harvard Medical School, Boston, MA 02115, USA. [2]Howard Hughes Medical Institute and Department of Biochemistry and Molecular Biology, Colorado State University, Fort Collins, CO 80523–1870, USA. [3]Department of Cancer Biology, Dana-Farber Cancer Institute and Harvard Medical School, Boston, MA 02115, USA. [4]Department of Biological Chemistry and Molecular Pharmacology, Harvard Medical School, Boston, MA 02115, USA.

*These authors contributed equally to this work.
†To whom correspondence should be addressed. E-mail: kkaye@rics.bwh.harvard.edu

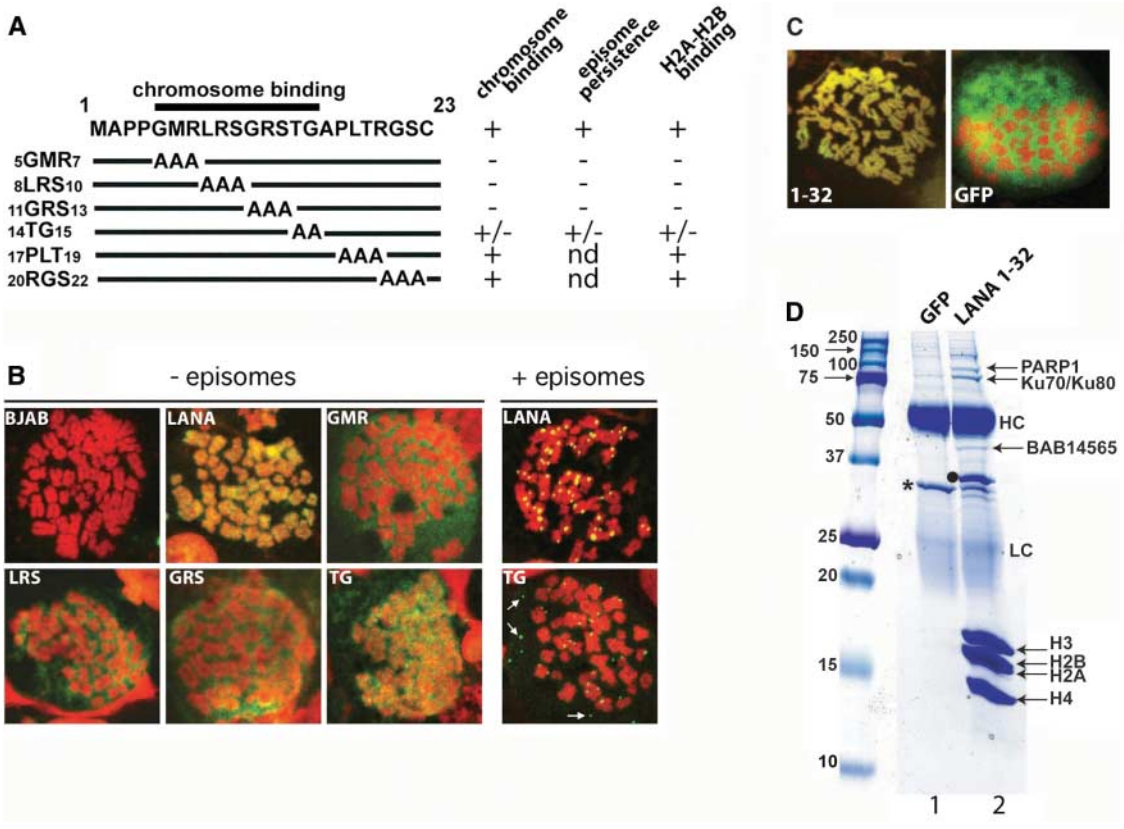

Fig. 1. LANA N terminus chromosome binding. (**A**) LANA scanning alanine mutants with summaries for chromosome binding, episome persistence (*7*), and H2A-H2B binding. nd, not determined. (**B**) Metaphase spreads of BJAB cells and BJAB cells stably expressing LANA, $LANA_5GMR_7$, $LANA_8LRS_{10}$, $LANA_{11}GRS_{13}$, or $LANA_{14}TG_{15}$. Overlay of LANA (green) and chromosomes (red) generates yellow. Cells containing KSHV episomes are indicated. Arrows denote $LANA_{14}TG_{15}$ dots that have detached from chromosomes. Magnification is 630×. (**C**) Metaphase BJAB cells stably expressing GFP NLS or GFP LANA 1-32 at 630× magnification. (**D**) Proteins co-precipitating with GFP LANA 1-32 (lane 2) were identified after resolution in a 4 to 16% gradient gel. HC, heavy chain; LC, light chain; asterisk, GFP; ●, GFP LANA 1-32. The stoichiometry of histones within nucleosomes and their arginine-rich nature contribute to the intense histone Coomassie staining. Numbers on the left-hand side of the gel are size markers (kD).

respectively) associates with chromosomes (Fig. 1A). LANA with alanine substitutions at residues $_{14}TG_{15}$ (termed LANA $_{14}TG_{15}$) may have reduced affinity for chromosomes (*7*). To further investigate LANA $_{14}TG_{15}$, we stably expressed these mutants in uninfected BJAB cells at amounts similar to those of LANA in infected PEL cells. LANA (green) tightly associated with chromosomes (red) (overlay generates yellow), whereas LANA $_5GMR_7$, LANA $_8LRS_{10}$, and LANA $_{11}GRS_{13}$ (green) did not (Fig. 1B). LANA $_{14}TG_{15}$ (green) associated with chromosomes (red) (overlay generates yellow) but also distributed between chromosomes, indicating weak association. We also investigated LANA $_{14}TG_{15}$ chromosome association in cells with KSHV episomes. In contrast to its broad distribution over chromosomes in the absence of KSHV episomes, LANA concentrates to dots along mitotic chromosomes at sites of episomes, consistent with its role in tethering KSHV DNA to chromosomes (*5*, *12*). Although LANA dots always tightly associated with chromosomes, ~30% of mitotic cells had LANA $_{14}TG_{15}$ dots that were detached from chromosomes (Fig. 1B, arrows). Because LANA dots are sites of KSHV DNA, $LANA_{14}TG_{15}$ dots not associated with chromosomes indicate inefficient episome partitioning. This finding follows our previous observation that LANA $_{14}TG_{15}$ is deficient in supporting episome persistence (*7*).

To identify N-terminal LANA's mitotic chromosome binding partner, we affinity-purified interacting proteins. BJAB cells stably expressing green fluorescent protein (GFP) fused to LANA residues 1 to 32 (GFP LANA 1-32), or GFP fused with a nuclear localization signal (GFP NLS), were generated (Fig. 1C). GFP does not affect LANA's chromosome localization (*7*) or negate its ability to mediate episome persistence (*13*). Proteins that interacted specifically with GFP LANA 1-32 were identified by co-immunoprecipitation followed by mass spectrometry (Fig. 1D). These included large amounts of core histones H2A, H2B, H3, and H4, as well as Ku70, Ku80, poly(adenosine diphosphate-ribose) polymerase 1 (PARP1), and BAB14565, a protein with high homology to the histone variant macroH2A. We determined with the use of knockout mouse embryo fibroblasts (MEFs) that Ku70, Ku80, and PARP1 do not mediate LANA chromosome association [fig. S1 and Supporting Online Material (SOM) Text].

The diffuse distribution of the LANA N terminus over mitotic chromosomes and the efficient precipitation of core histones strongly suggested that core histones mediate LANA chromosome docking. To further investigate this possibility, we assayed whether N-terminal LANA bound histones during mitosis. GFP LANA 1-32 was immunoprecipitated from asynchronous cells (~5% mitotic) (Fig. 2A, lane 2) or from metaphase-arrested cells (~85% mitotic) (Fig. 2A, lane 5). Despite the 17-fold difference in mitotic index, core histones precipitated similarly from asynchronous and metaphase-arrested cells. These results indicate that LANA associates with core histones throughout most or all of the cell cycle.

We determined whether full-length LANA also associated with core histones. GFP LANA 1-32 and GFP LANA, but not GFP NLS, efficiently precipitated core histones after expression in COS cells (Fig. 2B). We also investigated LANA's association with core histones in KSHV-infected BCBL-1 PEL cells. After incubation with a monoclonal antibody against LANA or with polyclonal serum, histone H2B was precipitated from BCBL-1 cells but not uninfected BJAB cells (Fig. 2C). Therefore, LANA interacts with core histones in KSHV-infected tumor cells.

We investigated whether the LANA N terminus directly binds nucleosome core particles (NCPs), which consist of two copies each of core histones H2A, H2B, H3, and H4, organizing ~147 base pairs (bp) of DNA (*14*). Glutathione *S*-transferase (GST) LANA 1-23, but not GST, directly bound and precipitated purified nucleosomes (Fig. 2D). Further, GST LANA 1-23 supershifted recombinant nucleosomes in a native gel (Fig. 2E). Because GST LANA 1-23 does not interact with purified DNA (*15*), binding was specific to the histone component of nucleosomes.

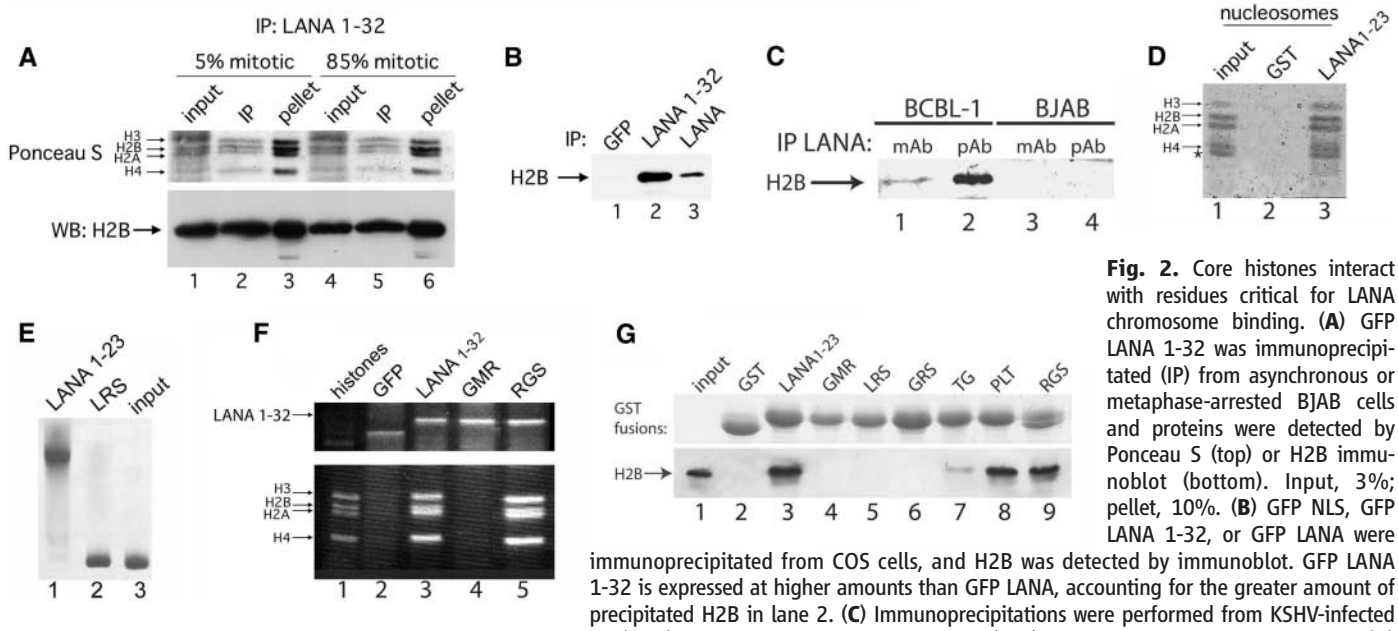

Fig. 2. Core histones interact with residues critical for LANA chromosome binding. (**A**) GFP LANA 1-32 was immunoprecipitated (IP) from asynchronous or metaphase-arrested BJAB cells and proteins were detected by Ponceau S (top) or H2B immunoblot (bottom). Input, 3%; pellet, 10%. (**B**) GFP NLS, GFP LANA 1-32, or GFP LANA were immunoprecipitated from COS cells, and H2B was detected by immunoblot. GFP LANA 1-32 is expressed at higher amounts than GFP LANA, accounting for the greater amount of precipitated H2B in lane 2. (**C**) Immunoprecipitations were performed from KSHV-infected BCBL-1 cells or uninfected BJAB cells by using monoclonal antibody (mAb) against LANA or polyclonal serum (pAb). H2B was detected by immunoblot. (**D**) H1-depleted nucleosomes were incubated with GST or GST LANA 1-23, and precipitated histones were detected by Coomassie. Input, 30%. Asterisk, degradation product. (**E**) Nucleosomes were incubated with GST LANA 1-23 or GST LANA 1-23 $_{8}$LRS$_{10}$, resolved by 5% native polyacrylamide gel electrophoresis, and detected by Coomassie. (**F**) Proteins immunoprecipitated by GFP or GFP fusions were detected by SYPRO Ruby (Invitrogen). Lane 1, purified histones. (**G**) GST fusion proteins were incubated with H1-depleted nucleosomes. GST fusions were detected by Coomassie, and precipitated H2B was detected by immunoblot.

We next investigated whether core histones interact with LANA residues necessary for chromosome association. GFP LANA 1-32 and GFP LANA 1-32 $_{20}$RGS$_{22}$, which associate with chromosomes, precipitated core histones from COS cells, whereas GFP LANA 1-32 $_{5}$GMR$_{7}$, which does not associate with chromosomes, did not (Fig. 2F). Further, GST LANA 1-23 $_{17}$PLT$_{19}$ and GST LANA 1-23 $_{20}$RGS$_{22}$ bound purified nucleosomes and nucleosomes from BJAB cell extracts (Fig. 2G and fig. S2). In contrast, GST LANA 1-23 $_{5}$GMR$_{7}$, GST LANA 1-23 $_{8}$LRS$_{10}$, and GST LANA 1-23 $_{11}$GRS$_{13}$, substituted at residues essential for chromosome binding, did not bind histones (Fig. 2, E and G, and fig. S2). Full-length LANA substituted at residues essential for chromosome binding also did not bind core histones (fig. S3). GST LANA 1-23 $_{14}$TG$_{15}$ bound nucleosomes at a reduced amount (Fig. 2G and fig. S2), similar to the reduced chromosome binding with this mutation (Fig. 1B). Thus, the same LANA residues are critical for histone and chromosome binding, providing strong evidence that core histones mediate LANA chromosome attachment.

We next investigated through which histones the LANA N-terminal region binds nucleosomes. GST LANA 1-23 and GST were incubated with acid-extracted histones, which contain core histone H2A-H2B dimers and H3-H4 tetramers. GST LANA 1-23 precipitated histones H2A and H2B, but not H3 and H4 (Fig. 3A). GST did not bind histones. Antibody that detects both histones H1 and H2B confirmed the H2B binding and demonstrated that GST LANA 1-23 does not bind linker histone H1 (Fig. 3B). We also investigated whether LANA bound the tails or folded domain of H2A-H2B. GST LANA 1-23 precipitated both recombinant full-length H2A-H2B and tailless H2A-H2B (Fig. 3C). These results indicate that the LANA N terminus specifically binds nucleosomes through the folded domain of H2A-H2B.

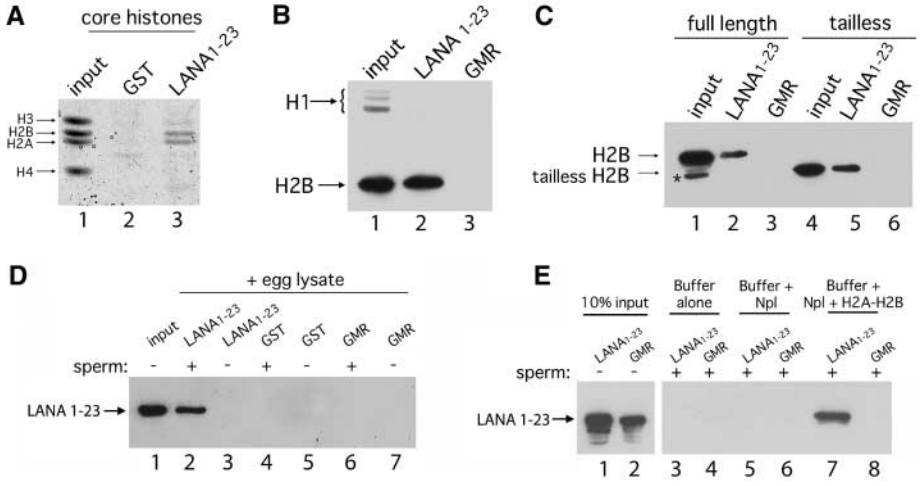

Fig. 3. Histones H2A-H2B are essential for LANA N-terminal chromosome binding. (**A**) GST or GST LANA 1-23 was incubated with purified histones, and bound histones were detected by Coomassie. Lane 1, 30% input. (**B**) GST LANA 1-23 or GST LANA 1-23 $_{5}$GMR$_{7}$ was incubated with purified histones, and precipitated H1 and H2B were detected by immunoblot. Lane 1, 30% input. (**C**) GST LANA 1-23 or GST LANA 1-23 $_{5}$GMR$_{7}$ was incubated with full-length or tailless H2A-H2B dimers, and precipitated H2B was detected by immunoblot. Input, 30%. Asterisk, degradation product. (**D**) GST, GST LANA 1-23, or GST LANA 1-23 $_{5}$GMR$_{7}$ was incubated in egg lysate HSS with or without *Xenopus* sperm chromatin, and chromatin-bound GST proteins were detected by immunoblot. Input, 10%. (**E**) GST LANA 1-23 or GST LANA 1-23 $_{5}$GMR$_{7}$ was incubated with *Xenopus* sperm chromatin in buffer alone, with purified nucleoplasmin (Npl), or with nucleoplasmin plus H2A-H2B dimers. Chromatin-bound GST proteins were detected.

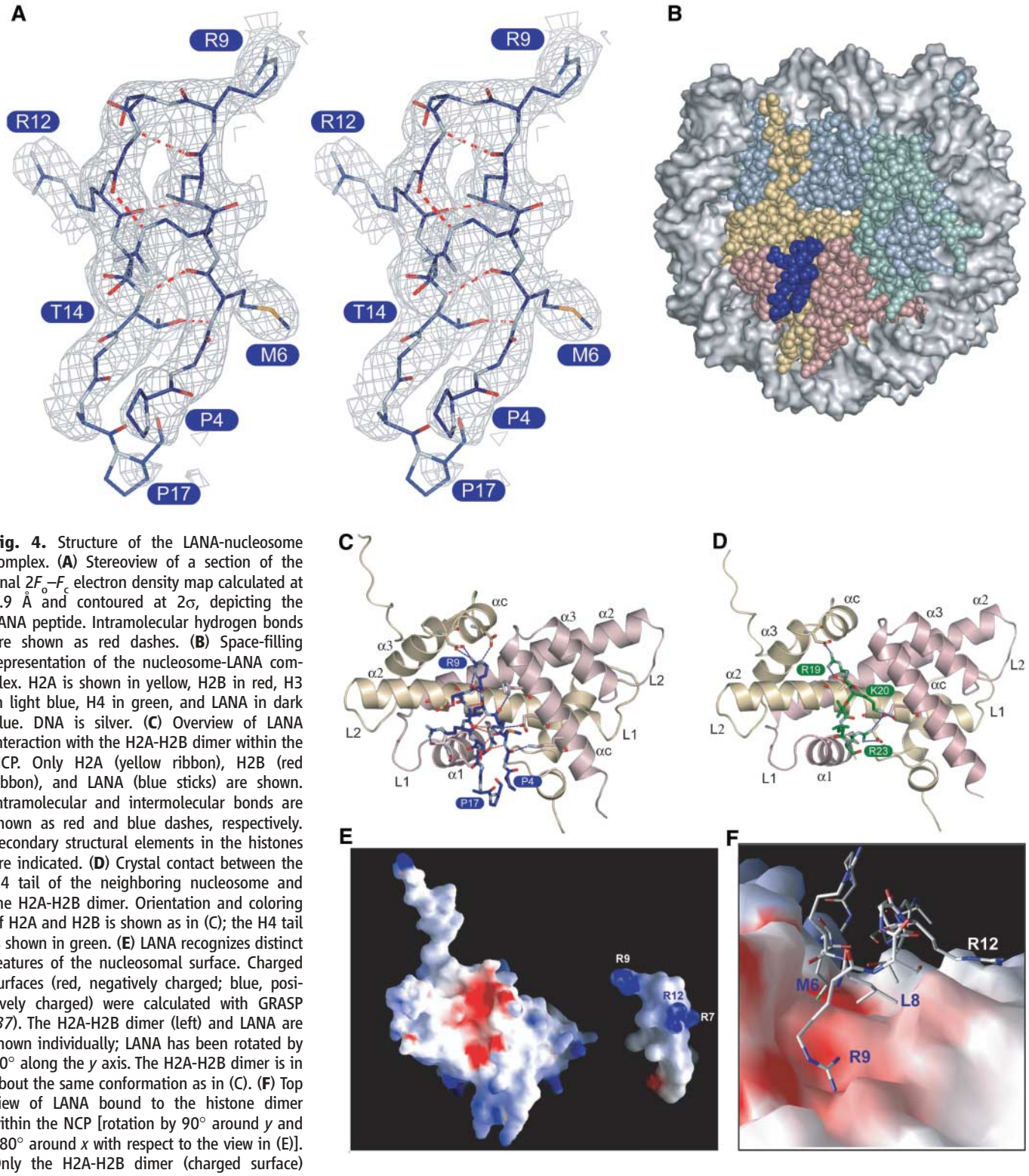

Fig. 4. Structure of the LANA-nucleosome complex. (**A**) Stereoview of a section of the final $2F_o–F_c$ electron density map calculated at 2.9 Å and contoured at 2σ, depicting the LANA peptide. Intramolecular hydrogen bonds are shown as red dashes. (**B**) Space-filling representation of the nucleosome-LANA complex. H2A is shown in yellow, H2B in red, H3 in light blue, H4 in green, and LANA in dark blue. DNA is silver. (**C**) Overview of LANA interaction with the H2A-H2B dimer within the NCP. Only H2A (yellow ribbon), H2B (red ribbon), and LANA (blue sticks) are shown. Intramolecular and intermolecular bonds are shown as red and blue dashes, respectively. Secondary structural elements in the histones are indicated. (**D**) Crystal contact between the H4 tail of the neighboring nucleosome and the H2A-H2B dimer. Orientation and coloring of H2A and H2B is shown as in (C); the H4 tail is shown in green. (**E**) LANA recognizes distinct features of the nucleosomal surface. Charged surfaces (red, negatively charged; blue, positively charged) were calculated with GRASP (*37*). The H2A-H2B dimer (left) and LANA are shown individually; LANA has been rotated by 90° along the *y* axis. The H2A-H2B dimer is in about the same conformation as in (C). (**F**) Top view of LANA bound to the histone dimer within the NCP [rotation by 90° around *y* and 180° around *x* with respect to the view in (E)]. Only the H2A-H2B dimer (charged surface) and LANA (stick model) are shown.

We wished to demonstrate directly that the LANA N terminus uses H2A-H2B to bind chromosomes. We used *Xenopus laevis* sperm chromatin, which is naturally deficient in H2A-H2B and instead contains sperm-specific basic proteins X and Y. In addition, *Xenopus* sperm lack H1 (*16*–*18*). Upon incubation with high-speed supernatant (HSS) from *Xenopus* egg lysate, egg cell–derived nucleoplasmin protein mediates sperm chromatin decondensation and replacement of X and Y with egg H2A-H2B dimers. To verify LANA chromosome binding in this system, we incubated HSS-treated chromatin, which contains wild-type H2A-H2B dimers, with GST fusions. GST LANA 1-23 bound sperm chromatin that had undergone H2A-H2B deposition through HSS treatment, but GST LANA 1-23 $_5$GMR$_7$ and GST did not (Fig. 3D). No LANA protein precipitated in the absence of chromatin. Therefore, N-terminal LANA binds *Xenopus* chromosomes after H2A-H2B deposition.

We stringently assayed whether H2A-H2B were required for LANA chromosome binding. HSS contains other factors in addition to H2A-H2B and nucleoplasmin. We therefore used a purified system with nucleoplasmin and recombinant H2A-H2B dimers in place of HSS. GST LANA 1-23 did not bind H2A-H2B-deficient sperm chromatin that had been treated with buffer or with purified nucleoplasmin alone. However, after incubation with nucleoplasmin and recombinant histone H2A-H2B dimers, which allows for deposition of histones H2A-H2B into sperm chromatin, GST LANA 1-23 specifically bound sperm chromatin (Fig. 3E). Thus, H2A-H2B is essential for LANA chromosome binding.

We solved the x-ray crystal structure of LANA residues 1 to 23 complexed with the NCP. Data collection and refinement statistics are summarized in table S1. Figure 4A shows a $2F_o–F_c$ map of the final model of the LANA peptide, contoured at 2σ. LANA forms a tight hairpin that is stabilized by five intramolecular hydrogen bonds (three β-type interactions and two side-chain or main-chain interactions) (Fig. 4, A and C) and by numerous hydrogen bonds and Van der Waals contacts with the nucleosomal surface.

Consistent with the biochemical experiments (Fig. 3, A to C), the LANA peptide interacts exclusively with the H2A-H2B dimer within the nucleosome (Fig. 4B). Histone fold regions and extensions of H2A and H2B are implicated in the interaction, but not the flexible histone tails. The hairpin is wedged between the αC and α1 helix of H2B (Fig. 4C); the turn of the hairpin abuts the H2A docking domain that forms a major interaction interface between the H2A-H2B dimer and the $(H3\text{-}H4)_2$ tetramer (*19*). The L1 loop of H2B as well as the α2 and α3 helices of H2A are also involved in LANA binding, consistent with the requirement for a folded H2A-H2B dimer for LANA binding. Molecular details of the interactions between LANA and the nucleosome are shown in fig. S4 (SOM Text). Substitution of individual LANA amino acids 5 to 16 demonstrated that residues important for chromosome association (fig. S5 and SOM Text) have critical roles in the interaction between LANA and the NCP. Of note, the overall structure of the nucleosome is maintained upon LANA binding (Fig. 4B).

Interactions of LANA with the NCP resemble those between the NCP and the H4 N-terminal tail from a neighboring nucleosome within the crystal lattice (Fig. 4D) (*20*). Both peptides interact with the same conserved acidic patch composed of several residues from H2A and H2B on the highly contoured nucleosomal surface (*21*). Despite a lack of sequence homology between the LANA peptide and the N-terminal tail, many of the targeted residues in H2A and H2B are the same (see, for example, LANA R_9 and H4 R_{19} in Fig. 4, C and D, respectively). The interaction shown in Fig. 4D is essential for nucleosome crystallization (*14*), and biophysical experiments have indicated a unique role for the H4 tail and acidic patch interaction in the formation of chromatin higher order structure (*22*, *23*).

Analysis of the molecular surfaces of both the LANA peptide and the H2A-H2B dimer demonstrates excellent shape and charge complementarity (Fig. 4E), indicating that the LANA N-terminal region has evolved to recognize this region within the NCP with high specificity. LANA R_9 and Ser_{10} point into the acidic pocket formed by H2A and H2B, and hydrophobic LANA residues are inserted deep into a cleft delineated by the αC helix of H2B (Fig. 4F). The LANA peptide interaction buries 1340 $Å^2$, well within the range that is considered to be a stable interaction (*24*), which is notable considering that only 14 residues of LANA contribute to the interaction. For comparison, the molecular surface buried by the H4 tail–NCP interaction (Fig. 4D) is only 680 $Å^2$ and contains larger cavities.

This work demonstrates that LANA's N-terminal chromosome association is mediated by H2A-H2B and not by the earlier proposed candidates methyl-CpG binding protein 2 (MeCP2) or H1 (*8*, *12*, *25*). It was previously reported that LANA did not associate with murine chromosomes unless human MeCP2 was co-expressed (*8*). In contrast, we found that LANA bound murine chromosomes (fig. S1); further, MeCP2 was not identified from our affinity purification. Histone H1 did not bind the LANA N terminus and was not required for LANA to bind *Xenopus* chromatin (Fig. 3, B and E). These results also differ from proposed chromosome binding mechanisms for other episome maintenance proteins: Epstein-Barr virus EBNA1 binds chromosomes through the nucleolar EBP2 protein or AT hooks, and bovine papillomavirus E2 binds through the bromodomain protein Brd4 (*26*–*28*).

This work may also link H2A-H2B binding to LANA's transcriptional regulatory effects (*29*, *30*). In fact, LANA transcriptional activity can be dependent on N-terminal chromosome association (*31*). An intriguing possibility is that LANA may affect transcription by regulating transient H2A-H2B removal from nucleosomes through complexes such as FACT or nucleosome assembly protein 1 (*32*, *33*). Histone modifications regulate transcription and may also affect LANA's affinity for nucleosomes and effects on chromatin, although experiments with bacterially expressed protein (Figs. 2 to 4) indicate that histone modifications are not required for binding.

This work indicates a role for H2A-H2B in LANA-mediated DNA replication and episome persistence, because these functions are dependent on N-terminal LANA chromosome binding (*7*). Interestingly, histone fusions have been used as an alternative method of targeting LANA and EBNA1 to chromosomes (*10*, *27*, *34*, *35*). Linker histone H1 in place of the LANA or EBNA1 chromosome association region permits episome persistence, whereas core histones (H2B and H3, respectively) do not, perhaps because of positional restrictions related to the covalent linkages. Of note, LANA has a C-terminal chromosome association domain, but it cannot rescue chromosome binding of N-terminal mutated LANA (Fig. 1B) (*7*–*10*); its role in episome persistence is currently under investigation. The distribution of H2A-H2B throughout chromosomes provides a platform through which LANA tethered episomes can efficiently segregate to progeny nuclei. Strategies that interrupt the interaction between LANA and H2A-H2B may provide effective treatment and prevention of KSHV-associated diseases.

The x-ray crystal structure shows that a hairpin formed by KSHV LANA residues 5 to 13 interacts with eukaryotic chromatin by binding to an acidic patch formed by H2A-H2B within the nucleosome. Thus, LANA has evolved to use the differentially charged and contoured surface of the nucleosome as a "docking station" for episome attachment. The concept of the nucleosomal surface (as opposed to the flexible histone tails) as an interaction platform has been proposed earlier (*14*, *22*, *36*–*38*); we now report the structure of a protein complexed with the nucleosome core. It appears that an important function of histones, in addition to maintaining interaction with other histones to form the octamer and compacting genomic DNA, is to maintain a distinct surface landscape that is used as a docking platform by cellular and viral factors. Such interactions may locally affect nucleosome dynamics and/or alter chromatin higher order structure, with profound implications for transcription of underlying DNA regions.

References and Notes

1. Y. Chang *et al.*, *Science* **266**, 1865 (1994).
2. P. S. Moore, Y. Chang, *N. Engl. J. Med.* **332**, 1181 (1995).
3. E. Cesarman, Y. Chang, P. S. Moore, J. W. Said, D. M. Knowles, *N. Engl. J. Med.* **332**, 1186 (1995).
4. J. Soulier *et al.*, *Blood* **86**, 1276 (1995).
5. M. E. Ballestas, P. A. Chatis, K. M. Kaye, *Science* **284**, 641 (1999).
6. L. L. Decker *et al.*, *J. Exp. Med.* **184**, 283 (1996).
7. A. J. Barbera, M. E. Ballestas, K. M. Kaye, *J. Virol.* **78**, 294 (2004).
8. A. Krithivas, M. Fujimuro, M. Weidner, D. B. Young, S. D. Hayward, *J. Virol.* **76**, 11596 (2002).
9. T. Piolot, M. Tramier, M. Coppey, J. C. Nicolas, V. Marechal, *J. Virol.* **75**, 3948 (2001).
10. H. Shinohara *et al.*, *J. Virol.* **76**, 12917 (2002).
11. Single-letter abbreviations for the amino acid residues are as follows: A, Ala; C, Cys; D, Asp; E, Glu; F, Phe; G, Gly; H, His; I, Ile; K, Lys; L, Leu; M, Met; N, Asn; P, Pro; Q, Gln; R, Arg; S, Ser; T, Thr; V, Val; W, Trp; and Y, Tyr.
12. M. A. Cotter 2nd, E. S. Robertson, *Virology* **264**, 254 (1999).
13. T. Tetsuka *et al.*, *Virus Genes* **29**, 175 (2004).
14. K. Luger, A. W. Mader, R. K. Richmond, D. F. Sargent, T. J. Richmond, *Nature* **389**, 251 (1997).
15. A. J. Barbera *et al.*, unpublished data.
16. A. Philpott, G. H. Leno, R. A. Laskey, *Cell* **65**, 569 (1991).
17. A. Philpott, G. H. Leno, *Cell* **69**, 759 (1992).

18. A. W. Murray, *Methods Cell Biol.* **36**, 581 (1991).
19. K. Luger, T. J. Richmond, *Curr. Opin. Genet. Dev.* **8**, 140 (1998).
20. C. A. Davey, D. F. Sargent, K. Luger, A. W. Maeder, T. J. Richmond, *J. Mol. Biol.* **319**, 1097 (2002).
21. K. Luger, T. J. Richmond, *Curr. Opin. Struct. Biol.* **8**, 33 (1998).
22. B. Dorigo, T. Schalch, K. Bystricky, T. J. Richmond, *J. Mol. Biol.* **327**, 85 (2003).
23. J. Y. Fan, D. Rangasamy, K. Luger, D. J. Tremethick, *Mol. Cell* **16**, 655 (2004).
24. S. Jones, J. M. Thornton, *Proc. Natl. Acad. Sci. U.S.A.* **93**, 13 (1996).
25. S. C. Verma, E. S. Robertson, *FEMS Microbiol. Lett.* **222**, 155 (2003).
26. J. You, J. L. Croyle, A. Nishimura, K. Ozato, P. M. Howley, *Cell* **117**, 349 (2004).
27. J. Sears *et al.*, *J. Virol.* **78**, 11487 (2004).
28. P. Kapoor, K. Shire, L. Frappier, *EMBO J.* **20**, 222 (2001).
29. A. Krithivas, D. B. Young, G. Liao, D. Greene, S. D. Hayward, *J. Virol.* **74**, 9637 (2000).
30. R. Renne *et al.*, *J. Virol.* **75**, 458 (2001).
31. L. Y. Wong, G. A. Matchett, A. C. Wilson, *J. Virol.* **78**, 10074 (2004).
32. G. Orphanides, G. LeRoy, C. H. Chang, D. S. Luse, D. Reinberg, *Cell* **92**, 105 (1998).
33. Y. J. Park, J. V. Chodaparambil, Y. Bao, S. J. McBryant, K. Luger, *J. Biol. Chem.* **280**, 1817 (2004).
34. J. L. Yates, N. Warren, B. Sugden, *Nature* **313**, 812 (1985).
35. S. C. Hung, M. S. Kang, E. Kieff, *Proc. Natl. Acad. Sci. U.S.A.* **98**, 1865 (2001).
36. R. K. Suto, M. J. Clarkson, D. J. Tremethick, K. Luger, *Nat. Struct. Biol.* **7**, 1121 (2000).
37. F. van Leeuwen, P. R. Gafken, D. E. Gottschling, *Cell* **109**, 745 (2002).
38. J. H. Park, M. S. Cosgrove, E. Youngman, C. Wolberger, J. D. Boeke, *Nat. Genet.* **32**, 273 (2002).
39. A. Nicholls, K. A. Sharp, B. Honig, *Proteins* **11**, 281 (1991).
40. HeLa nucleosomes were a gift of X. He, P. Pascual-Ahuir Giner, and R. Kingston. PARP1 and Ku80 knockout MEFs were generously provided by J. Jung and A. Nussenzweig, respectively. We thank P. Yiu for assistance with sperm chromatin experiments; E. Kieff for helpful discussions; P. Dyer, O. Peersen, and V. Srinivasan for technical assistance; R. Edayathumangalam and S. Chakravarthy for help with data collection and structure determination; and A. Straight and T. Mitchison for the plasmid encoding H2A-H2B used in the chromatin binding experiments. This work was supported by grant CA82036 (to K.M.K.) from the National Cancer Institute and grants GM067777 (to K.L.) and GM62267 (to J.C.W.) from the National Institute of General Medical Sciences. Coordinates have been deposited at the Protein Data Bank database (entry code 1ZLA).

Supporting Online Material
www.sciencemag.org/cgi/content/full/311/5762/856/DC1
Materials and Methods
SOM Text
Figs. S1 to S5
Table S1
References and Notes

26 September 2005; accepted 12 January 2006
10.1126/science.1120541

Neurochemical Modulation of Response Inhibition and Probabilistic Learning in Humans

Samuel R. Chamberlain,[1,3]* Ulrich Müller,[1,2,3] Andrew D. Blackwell,[1,3] Luke Clark,[2,3] Trevor W. Robbins,[2,3] Barbara J. Sahakian[1,3]

Cognitive functions dependent on the prefrontal cortex, such as the ability to suppress behavior (response inhibition) and to learn from complex feedback (probabilistic learning), play critical roles in activities of daily life. To what extent do different neurochemical systems modulate these two cognitive functions? Here, using stop-signal and probabilistic learning tasks, we show a double dissociation for the involvement of noradrenaline and serotonin in human cognition. In healthy volunteers, inhibition of central noradrenaline reuptake improved response inhibition but had no effect on probabilistic learning, whereas inhibition of central serotonin reuptake impaired probabilistic learning with no effect on response inhibition.

Ascending monoamine projections play important neuromodulatory roles in high-level cognition through actions upon the prefrontal cortex (PFC), a major brain structure with considerable functional heterogeneity in humans (*1*). Dysfunction in these neurochemical systems is implicated in the etiology and psychopathology of psychiatric illnesses associated with cognitive deficits and PFC abnormalities, including depression, attention deficit–hyperactivity disorder (ADHD), obsessive-compulsive disorder (OCD), and drug addiction (*2*–*7*). Dopamine regulates executive functions dependent on the dorsolateral PFC, including working memory and attentional set-shifting, but the role of noradrenaline (NA) and serotonin [5-hydroxytryptamine (5-HT)] in cognition is less well characterized (*8*). The orbitofrontal cortex (OFC) is involved in emotion-cognition interactions, and 5-HT drugs modulate response to feedback and decision-making within this region (*9*–*15*). 5-HT and NA have both been implicated in response inhibition (*16*, *17*), a function that has been linked to the right inferior frontal gyrus (RIFG) (*18*).

We investigated the differential involvement of NA and 5-HT transmitter systems in these processes in humans, using the selective NA reuptake inhibitor (SNRI) atomoxetine and the selective 5-HT reuptake inhibitor (SSRI) citalopram. These agents are among the most selective inhibitors for brain NA and 5-HT reuptake transporters available for human use, according to in vitro and in vivo findings (*19*–*21*). Microdialysis studies in experimental animals have shown that acute systemic administration of atomoxetine rapidly increases PFC NA but not 5-HT and that the administration of citalopram rapidly increases PFC 5-HT but not NA (*19*, *22*). As such, these agents represent useful neurochemical tools for investigating the differential involvement of NA and 5-HT in human cognition.

Response inhibition, the ability to exert high-level inhibitory control over motor responses so as to suppress unwanted actions, can be assessed with the stop-signal procedure (*6*, *23*). In this procedure, volunteers are required to make rapid motor responses on Go trials but to inhibit responses if an auditory stop-signal occurs. By the infrequent nature of Stop trials, motor responses are made "prepotent." Response inhibition can be quantified by the stop-signal reaction time (SSRT), an estimate of the time taken to inhibit the prepotent motor response (*18*, *23*). Probabilistic learning refers to the ability to develop cognitive associations between stimuli and outcomes on the basis of punishing and rewarding feedback, and to modify these associations as appropriate (*12*). On probabilistic learning tasks, volunteers are required to select which of two stimuli they believe to be correct over a series of trials. After each choice, the computer provides punishing or rewarding feedback that is "degraded" (i.e., misleading on a subset of trials) (*12*).

The aim of the present study was to delineate the precise differential contribution of NA and 5-HT neurochemical systems to response inhibition and probabilistic learning. Sixty healthy male participants were recruited from the local community on the basis of being free from medical or psychiatric disorders according to assessment by a psychiatrist (mean age 25.7 ± SD 4.7 years, range 20 to 35) (*24*). Participants received single clinically relevant oral doses of atomoxetine (60 mg), citalopram (30 mg), or placebo in a double-blind parallel-groups design (*24*). Groups were matched for demographic characteristics (table S1). After spending 1.5 hours in a quiet waiting area to ensure drug

[1]Department of Psychiatry, University of Cambridge School of Clinical Medicine, Addenbrooke's Hospital, Box 189, Cambridge CB2 2QQ, UK. [2]Department of Experimental Psychology, [3]Behavioural and Clinical Neuroscience Institute, University of Cambridge, Cambridge CB2 3EB, UK.

*To whom correspondence should be addressed. E-mail: src33@cam.ac.uk